Investigation of passive and active silica-tin oxide nanostructured optical fibers fabricated by " inverse dip-coating " and " powder in tube " method based on the chemical sol-gel process and laser emission

Geoffroy Granger, Christine Restoin, Philippe Roy, Raphaël Jamier, Sébastien Rougier, Jean-René Duclere, André Lecomte, Romain Dauliat, Jean-Marc Blondy

Investigation of passive and active silica-tin oxide nanostructured optical fibers fabricated by "inverse dip-coating" and "powder in tube" method based on the chemical sol-gel process and laser emission

G. Granger[1], C. Restoin[2], P. Roy[2], R. Jamier[2], S. Rougier[2], J.-R. Duclere[3], A. Lecomte[3], R. Dauliat[2,4], J.-M. Blondy[2]

1 Institut für Strahlwerkzeuge (IFSW), 43 Pfaffenwaldring 70569 Stuttgart, Germany
2 Xlim Recherche Institut UMR-CNRS n°7252, 123 avenue Albert Thomas, 87060 Limoges Cedex, France
3 SPCTS UMR-CNRS n°7315, 12 rue Atlantis 87068 Limoges Cedex, France
4 Institute for Photonic Technology, 9Albert Einstein Straße, 07745 Jena, Germany

ABSTRACT

This paper presents a study of original nanostructured optical fibers based on the SiO_2-SnO_2-(Yb^{3+}) system. Two different processes have been developed and compared: the sol-gel chemical method associated to the "inverse dip-coating" (IDC) and the "powder in tube" (PIT) process. The microstructural and optical properties of the fibers are studied according to the concentration of SnO_2. X-Ray Diffraction as well as Transmission Electron Microscopy studies show that SnO_2 crystallizes into the cassiterite phase as nanoparticles with a diameter ranging from 4 to 50 nm as a function of tin oxide concentration. A comparative study highlights a better conservation of SnO_2 into the fiber core with the PIT approach according to the refractive index profile and X-Ray analysis measurement. The attenuation evaluated by the classic cut-back method gives respectively values higher than 3 dB/m and 0.2 dB/m in the visible (VIS) and infrared (IR) range for the PIT fiber whereas background losses reach 0.5 dB/m in the VIS range for IDC fibers. The introduction of ytterbium ions into the core of PIT fibers, directly in the first chemical step, leads to a laser emission (between 1050 and 1100 nm) according to the fiber length under 850 nm wavelength pumping. Luminescence studies have demonstrated the influence of the tin oxide nanostructure on the rare earth optical properties especially by the modification of the absorption (850 to 1000 nm) and emission (950 to 1100 nm) by discretization of the bands, as well as on the IR emission lifetime evaluated to 10 µs.

Keywords: Sol-gel, optical fiber, nanoparticles, tin oxide, laser emission.

1. INTRODUCTION

Recent years, researches on nanostructured optical fibers elaborated by incorporating dielectric (ZrO_2[1,2], MgO[3]), ceramic[4] (YAG[5], Y_2O_3[6]), semi-conductor[7], metallic nanoparticles (Au[8] or Cu[9]), or quantum dots[10] in an amorphous matrix have attracted much attention. These nanoparticles, dispersed in a silica matrix show original nonlinear optical properties[11-13] and offer a great potential for optical amplification as the rare earth (RE) ions[14,15] doping concentration can be higher than in an amorphous medium. Moreover, the energy transfer phenomenon can be observed in such RE doped nanoparticles that leads to exotica luminescence properties[16,17]. For example, zirconia nanoparticles have been successfully incorporated by the sol-gel "inverse dip-coating" (IDC) method[1] and the Modified Chemical Vapor Deposition (MCVD)[2] process: the laser effect has then been demonstrated in Yb^{3+} or Er^{3+}doped optical fiber[2,18]. The "powder in tube" technique (PIT) is used for original composition based on magnesium and silica[19]. However, only few realizations of nanocomposite fibers have been published and the incorporation of semiconductor nanoparticles in the core of an optical fiber is still a challenge considering the difficulties of the technological steps. Tin oxide appears as an interesting candidate because of its low phonon energy (630 cm^{-1}) and its high refractive index (1.99 at 632 nm). A study developed by Brambilla *et al.*[20] has allowed achieving a low tin oxide doped fiber by the MCVD method[21]. The tin atoms are here included in the silica network[22] as the SnO_2 concentration is quite low. Our aim is to obtain high doped SnO_2 core fiber, in order to enhance the optical properties of the tin oxide nanoparticles. This purpose cannot be achieved by the classical MCVD method due to the volatility of tin oxide. For this reason, the chemical sol-gel process appears as a very interesting alternative method. Indeed, it is a low temperature process which allows producing nanostructured SiO_2-SnO_2 compounds as well as thin films with a high control of the doping level[23] and a high purity.

In this work, we report on the realization of passive and active nanostructured fiber based on the SiO_2-SnO_2-(Yb^{3+}) system. The preform synthesis based on the chemical sol-gel method is first presented and the fiber elaboration by IDC and PIT is described. The microstructural and chemical analyses show the formation of pure SnO_2 nanoparticles. The characterization of the passive fiber demonstrates a modification of the core composition especially for the first process employed. The ytterbium ions doping in the PIT fiber leads to the first laser emission in this unconventional core composition. This effect will be discussed thanks to the microstructural and spectroscopic studies.

2. FABRICATION PROCESSES

The SiO_2-SnO_2 sols are prepared from tin (IV) n-propoxide (Alfa Aesar) and tetraethylorthosilicate (Alfa Aesar), as metal precursors. Isopropanol and nitric acid (HNO_3) are respectively used as solvent and catalyst to control the hydrolysis and condensation reactions. The tin alkoxide concentration varies from 20% mol (SN20) up to 90% mol (SN90) in order to study the influence of the chemical composition on the resulting SnO_2 nanoparticles size, spatial distribution and consequently optical properties of the fiber. A pure SiO_2 (SI) sol is elaborated under the same conditions as a comparative material. In the case of RE doping, the ultra-dry powder of ytterbium isopropoxide is added and dissolved under mechanical stirring (16 000ppm.mol: SN40_Yb). Then, the inverse dip coating process which is based on the deposition of sol-gel layers in a silica tube is developed to achieve the preforms and followed by the drawing fiber step[1]. The processing was achieved in a clean room to avoid dust pollution. All composition that have been drawn are labelled SNx_IDC (x=20 to 90). A part of each sol synthesized to fabricate the fibers is sampled, aged to gel and dried to obtain a xerogel which is then grinded into a fine powder. The same heat treatment is applied under air atmosphere on both SiO_2-SnO_2 layers and powders: 670 °C to eliminate the residual organic compounds and then 1000 °C to get the SnO_2 crystallization (around 450 °C) and the densification of the silica network. A second way of fabrication is then explored by using these powders based on the 30% (SN30_PIT) and 40% mol (SN40_PIT): the powder in tube process. The xerogel powders are inserted in a silica tube which is then drawn into an optical fiber. Finally the active fiber (SN40_Yb_PIT), based on the SN40_Yb powder, is drawn in the same conditions. A powder based on pure silica realized in the same condition and identical ytterbium concentration has been achieved to get comparative element for the spectroscopic study (SI_Yb).

3. MICROSTRUCTURAL INVESTIGATIONS

The studies of microstructural properties has been performed using high X-Ray Diffraction (XRD)[24] and Transmission Electron Microscopy (TEM). The chemical analysis is achieved by X-Ray analysis (EDX). The XRD patterns corresponding to the xerogel powders for the various compositions (SNx, x=20 to 90) are presented on fig. 1 and compared to the SI powder.

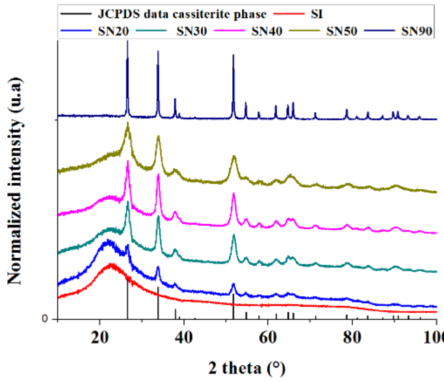

Figure 1. XRD patterns of SNx (x=20 to 90) powders compared to SI powder. The patterns are arbitrary shifted for clarity.

The position of the XRD peaks, according to the JCPDS data, indicated that the SnO_2 nanocrystallites are in the cassiterite phase and embedded in an amorphous SiO_2 matrix. The size of the crystal varies from 4 to 50 nm for tin oxide concentration ranging from 20 to 90 mol% (evaluated by Scherrer's formula). These values are in rather good agreement with the crystallite size previously observed by Wu *et al.*[23] or Van Tran *et al.*[25] on SiO_2-SnO_2 nanocomposite thin films and are also confirmed by TEM studies on the powder SN20 (fig. 2a) and SN40 (Fig. 2c).

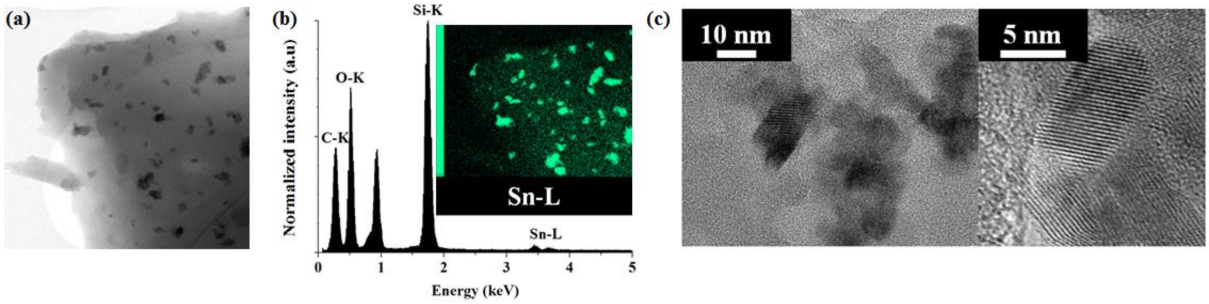

Figure 2. (a) TEM picture of SN20 powder. (b) EDX measurements on a single particle of the SN20 powder; inset : Sn mapping of the SN20 powder. (c) TEM picture of SnO_2 nanoparticle in the SN40 powder.

However, it is important to note that when the SnO_2 concentration reaches 90%, the Scherrer's formula became tendentious so the value of 50 nm has to be considered with caution. We can observe that the width of the peak decreases when the SnO_2 concentration increases, which means that the crystallite dimensions increase with the concentration. The EDX mapping measurements on the SN20 powder (inset fig. 2b) shows that these NP are composed of SnO_2 embedded in an amorphous silica medium (fig. 2b).

4. INVESTIGATION OF OPTICAL PROPERTIES

4.1 Passive fibers realized by the IDC process

First of all, the fibers elaborated by IDC have been characterized. The refractive index (RI) has been evaluated by a commercial profiler at 668 nm wavelength. The analysis of the nanostructured core fiber RI profiles shows that the RI is quite constant and equal to 1.4573 while the starting SnO_2 core composition increases from 20 % to 90 % mol (fig. 3a). Moreover, this value is greatly lower than the expected one calculated by the Lorenz-Lorentz equation[26] that gives a value from 1.666 to 1.911 for the studied compositions considering the theoretical RI equal to 1.99 and 1.456 for SnO_2 and SiO_2 respectively. However, this model can only be used to get an approximation of the real RI. Indeed, Van Tran *et al.*[24] have measured a refractive index around 1.608 on a 70 % mol SiO_2 and 30 % mol SnO_2 thin films elaborated by the sol-gel process and heat treated at 1200 °C. This difference with the theoretical values probably comes from the overvaluation of the theoretical density. Nevertheless, the knowledge of the refractive index leads to estimate the SnO_2 concentration in the core of the fibre. In our case, the tin oxide concentration is estimated around 3400 ppm mol in the core. The difference with the initial concentration is linked to a loss of tin oxide probably by evaporation during the fiber drawing step on one hand, facilitated by the large exchange surface inside the preform. On the over hand, the Gaussian shape of the refractive index profile also indicates that Sn atoms diffuse towards the cladding during the fiber drawing process.

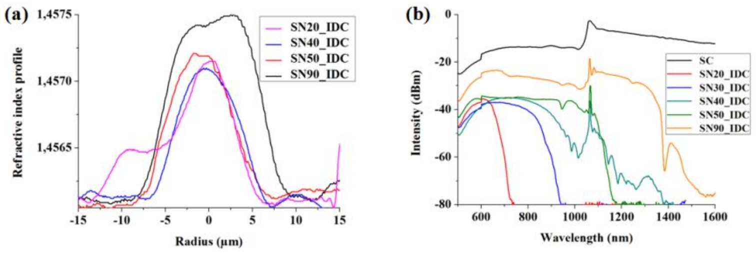

Figure 3. (a) RIP of the SNx_IDC (x=20 to 90). (b) Transmission spectra of the SNx_IDC (x=20 to 90) fibers and the SC source.

The transmission spectra of the fibers have been achieved thanks to a super-continuum white light source (SC) (fig. 3b). In this way, we observe a large transmission band that increases as a function of the RIP. For the SN50_IDC and SN90_IDC fiber, we can note two absorption peaks: the first one, at a 950 nm wavelength and the other one at a 1250 nm wavelength correspond to the coupling between OH fundamental mode and the SiO_4 tetrahedron vibrations[27]. The OH peak at a 1390 nm wavelength is observed and is linked to the chemical synthesis[27]. The optical losses are evaluated by the classical cut-back method and are lower than 1 dB/m in the visible range for each sample (0.5 dB/m at λ=650 nm). According this low RIP, these fibers are very bending sensitive.

4.2 Fibers realized by the PIT method

In a second step, the fibers elaborated by the PIT process are explored in order to limit the tin oxide evaporation. The RIP of the core presented on the fig. 4a shows a difference of the refractive index during the drawing process. It appears that the concentration of SnO_2 is lower in the fiber core the long time that the preform stays in the furnace in order to formed the drop part.

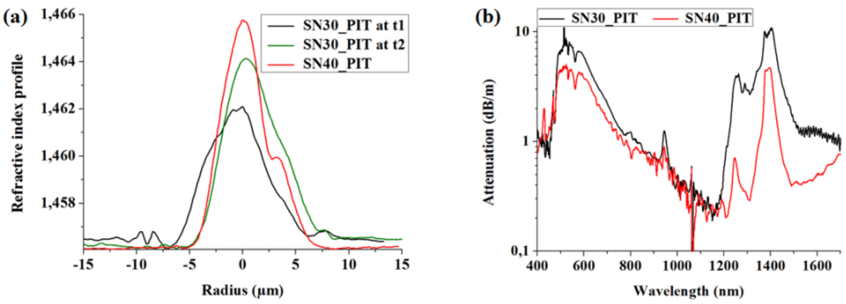

Figure 4. (a) RIP of the fiber SN30_PIT at two different longitudinal positions in the fiber and the SN40_PIT. (b) Attenuation spectra of SN30_PIT and SN40_PIT fiber.

Two phenomena can explain this RIP difference : tin oxide is evaporated at t1and is then trapped upper in the preform in the inter granular pores and thus kept into the core at t2, contrary to the IDC method where SnO is evaporated thanks to the large exchange surface ; recondensing process should also locally occur. The RIP maxima values are higher than these ones obtained with the IDC fiber but are still lower than those expected. At this concentration, we reach the limit of SnO_2 clustering which is thus conserved under nanocristallite[28]. The calculation, according to the EDX analysis shows that Sn concentration reaches 2 % where the signal was not detected for the IDC fiber. The PIT method is then chosen to achieve a high tin oxide concentration doped ytterbium fiber: Sn40_Yb_PIT. The RIP of this fiber is given in the fig. 5a. It appears that the RIP is larger than the passive PIT fiber. The role of the Yb^{3+} ions in this observation must be investigated much deeper. A RIP longitudinal study has to be done in order to compare the thermal effect with the passive ones. The EDX analysis gives then a Sn concentration around 5,8 % weight (fig. 5b).

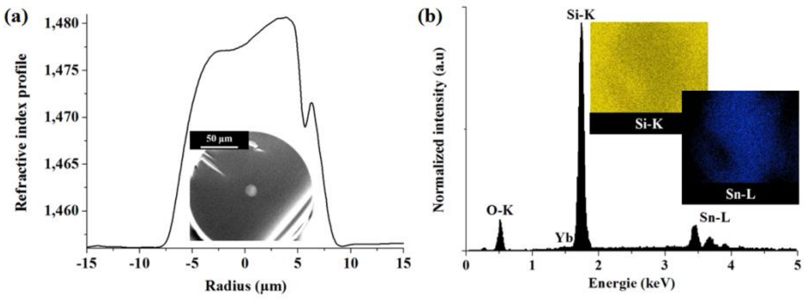

Figure 5. (a) RIP of the active fiber SN40_Yb_PIT with in inset the SEM fiber picture. (b) Signal record by EDX on the SN40_Yb_PIT core fiber with in inset the mapping of Si and Sn in the core region.

It appears that the attenuation presented on fig. 4b is quite different compared to fibers achieved by the IDC process. The absorption bands cannot be directly correlated to the intrinsic semiconductor properties as the SnO_2 band gap is around 3.6 eV (λ = 345 nm)[29]. The large attenuation band from visible range to 1 µm can be attributed to Raleigh diffusion of the SnO_2 particles[30]. Moreover, the near IR losses are as weak as 1 dB/m with a minimum between 1 and 1.3 µm (0.2 dB/m at λ=1200 nm). The PIT process allows achieving higher SnO_2 concentration in the core of the fiber and then a better transmission in the NIR band with low loss; this observation constitutes a motivation for doping with rare earth ions. The absorption characterization realized with a continuous white light source (SB) shows two absorption peaks: around 500 and 1200 dB/m respectively at 915 and 976 nm. At this RE concentration it is difficult to get a precise measure and this result from an average value. We cannot conclude on the ytterbium concentration because we have no information about the absorption cross section. For sake of clarity on the role of the Yb^{3+}, a measurement of the absorption cross section must be additionally performed. Then, the characterized fiber sample are short (some centimeter) that is not efficient to extract all the light from the clad and although the injection was made on the fundamental mode, the overlap factor (inset fig. 6a) is not perfect.

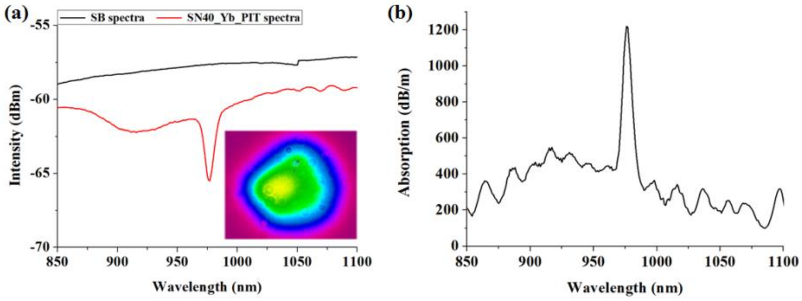

Figure 6. (a) Transmission spectra along a short piece of SN40_Yb_PIT fiber with in inset the output intensity beam pattern. (b) Average absorption measured on SN40_Yb_PIT fiber.

4.3 Spectroscopic powder characterization, influence of SnO_2 nanoparticles on the Yb^{3+} optical properties

The spectroscopic optical properties of the SN40_Yb powder has been achieved with a spectrometer Varian Cary 5000 that cover from 175 to 3000 nm spectral range. The absorption and emission spectra of SN40_Yb and SI_Yb powder are given in the fig. 8a in order to understand the influence of the tin oxide environment on the ytterbium luminescence properties. The SnO_2 band gap absorption appears around 350 nm[29] and the OH group spectral signature is around 1380 and 1250 nm for the both powders. The absorption around 1150 nm, common of the two powders could be linked to the nitric acid utilization, but no study to our knowledge refers to this. It is important to note that the 945 nm peak in the Sn40_Yb powder does not appear on the pure silica based powder, excluding the Si-OH bonds as origin of it. Moreover, it shows the influence of the SnO_2 nanoparticles on the Yb^{3+} optical properties. No peak appears in the red spectral range, which means that Yb^{2+} is not created during the process[31,32].

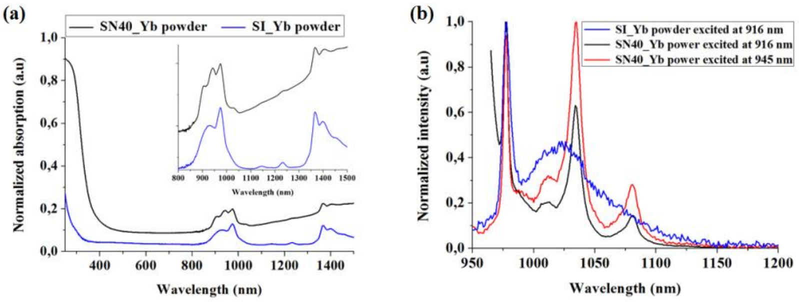

Figure 7. (a) SN40_Yb powder absorption spectra compared to the SI_Yb powder with in inset the zoom on the 800-1500 nm spectral range. (b) Photoluminescence spectra of the SN40_Yb powder compared to the SI_Yb powder for different excitation wavelengths.

The luminescence of SN40_Yb powders (fig. 7a) presents thinner emission compared to the SI_Yb. The preliminary study shows a shorter life time (around 10 µs) for this emission than the classical of 800 µs in silica network. This reduction is thus link the SnO_2 nanoparticles environment but also to the large OH amount well knows to participate to this phenomenon.

4.3 Characterization of Yb^{3+} doped fibers in laser regime

The laser experiment is based on a Fabry-Perot cavity composed of an input dichroic mirror, in charge of extracting the emitted radiation, and a metallic one, closing the cavity. The fiber is pumped by an tunable continuous Ti:Saph laser (fig. 8a). The pumping wavelength is fixed at 850 nm in order to get higher available pump power. The spectra recorded for different lengths of Sn40_Yb_PIT fiber are given in the fig. 8b. We obtain 8% efficiency slope (fig. 8c) for the emission around 1050 nm with a short 20.5 cm fiber length. According to the fiber length, the emission spectrum shifts to the higher wavelength to reach 1090 nm when the fiber length is about 1 m (fig. 8b).

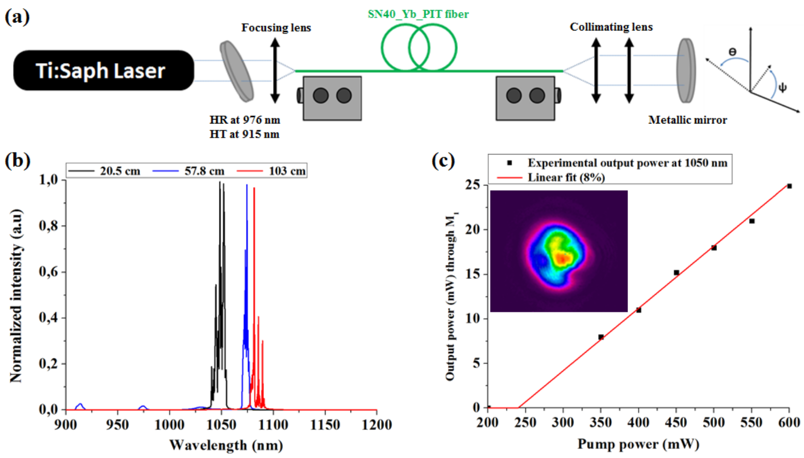

Figure 8. (a) Setup scheme of the laser characterization. (b) Normalized emission spectrum in active SN40_Yb_PIT fiber pumped at 850 nm according to the fiber length. (c) Slope of efficiency for the 1050 nm laser emission with in inset the near field intensity pattern of the output laser beam.

This low efficiency can be explained by several deleterious parameters as the core shape (inset fig. 8c) that make difficult the optical retroaction. Moreover, the large OH group amount of well-known to add losses and the pump wavelength which can be optimized could restrict the laser efficiency.

5. CONCLUSION

These fibers, realized by two different methods demonstrated the pertinence of the sol-gel process in order to achieved exotic composition based on semi-conductor. The development of an alternative process based on the powder in tube leads to a better conservation of the SnO_2 into the core of the optical fiber given thus a larger refractive index. The laser emission has been demonstrated for the first time to our knowledge from 1050 to 1090 nm for high ytterbium concentration. The optimization of the pump wavelength and of the heat treatment condition, especially in term of -OH group suppressing, should lead to better laser efficiency. The preliminary results in the spectral and time spectroscopic range show the influence of the SnO_2 nanoparticles environment on the rare earth. Thorough studies will be now developed according to the precursor ratio in order to understand the precise role of the tin oxide on the rare earth properties. The confirmation of the core nanostructuration especially by transmission electron microscopy or by guiding Raman microscopy would allow us to conclude. This work constitutes a milestone toward the realization of laser fiber with an unconventional core composition.

REFERENCES

[1] G. Brasse, C. Restoin, J.-L. Auguste, S. Hautreux, J.-M. Blondy and A. Lecomte, "Nanostructured optical fiber by the sol-gel process in the SiO_2-ZrO_2 system", Appl. Phys. Lett. **91**, 121920 (2007).
[2] A. V. Kir'yanov, M. C. Paul, Yu. O. Barmenkov, S. Das, M. Pal, S. K. Bhadra, L. Escalante Zarate, and A. D. Guzman-Chavez, "Fabrication and characterization of new Yb-doped zirconia-germano-alumino silicate phase-separated nano-particles based fibers", Opt. Soc. America **19**, 14823 (2011).
[3] W. Blanc, C. Guillermier and B. Dussardier, "Composition of nanoparticles in optical fibers by Secondary Ion Mass Spectrometry", Opt. Mat. Lett. **2**, 1504 (2012).
[4] B. N. Samson, P. A. Tick and N. F. Borrelli, "Efficient neodymium-doped glass ceramic fiber laser and amplifier", Opt. Lett. **26**, 145 (2001).
[5] M. C. Paul, S. Bysakh, S. Das, S. K. Bhadra, M. Pal, S. Yoo, M. P. Kalita, A. J. Boyland,J. K. Saju, "Yb_2O_3-doped YAG nano-crystallites in silica-based core glass matrix of optical fiber preform", Mat. Science and Engineer. B **175**, 108 (2010).
[6] S. Yoo, M. P. Kalita, A. J. Boyland, A. S. Webb, R. J. Standish, J. K. Sahu, M. C. Paul, S. Das, S. K. Bhadra and M. Pal, "Ytterbium-doped Y_2O_3 nanoparticle silica optical fibers for high power fiber lasers with supressed photodarkening", Opt. Com. **283**, 3423 (2010).
[7] G. Granger, C. Restoin, P. Roy, R. Jamier, S. Rougier, A. Lecomte and J.-M. Blondy, "Nanostructured optical fibers in the SiO_2/SnO_2 system", Mat. Lett. **120**, 292 (2014).
[8] A. Lin, D. H. Son, I. H. Ahn, G. H. Song and W.-T. Han, " Visible to infrared photoluminescence from gold nanoparticles embedded in germano-silicate glass fiber", Opt. Express **15**, 6374 (2007).
[9] H. El Hamzaoui, Y. Ouerdane, L. Bigot, G. Bouwmans, B. Capouen, A. Boukenter, S. Girard and M. Bouazaoui, "Sol gel derived ionic copper doped microstructured optical fiber a potential", Opt. Express **20**, 29571 (2012).
[10] A. Bhardwaj, A. Hreibi, L. Chao, J. Heo, J. August, J.-M. Blonby, "PbS quantum dots doped glass fibers for optical applications", CLEO US (2012).
[11] A. Clementi, N. Chiodini and A. Paleari, "Cubic optical nonlinearity in nanostructured SnO_2:SiO_2", Appl. Phys. Lett. **84**, 960 (2004).
[12] L. Bigot, H. El Hamzaoui, A. Le Rouge, G. Bowmans, F. Chassagneux, B. Capoen and M. Bouazaoui, "Linear and nonlinear optical properties of gold nanoparticle-doped photonic crystal fiber", Opt. Lett. **19**, 19061 (2011).

[13] A. Lin, B. H. Kim, S. Ju and W.-T. Han, "Fabrication and third-order nonlinearity of germane-silicate glass fiber incorporated with Au nanoparticles", Proc. SPIE 6481, 1-7 (2007).
[14] M. Fukushima, N. Managaki, M. Fujii, H. Yanagi and S. Hayashi, "Enhancement of 1.54 μm emission from Er-doped sol-gel SiO_2 films by Au nanoparticles doping", J. Appl. Phys. **98**, 024316 (2005).
[15] C. Strhohhöfer and A. Polman, "Silver as a sensitizer for erbium", Appl. Phys. Lett. **81**, 1414 (2002).
[16] S. Brovelli, N. Chiodini, A. Lauria, F. Meinardi and A. Paleari, "Kinetics of luminescence of interface defects and resonant Er^{3+} ions in nanostructured SnO_2:SiO_2", Solid State Communication **138**, 574 (2006).
[17] C. Bouzidi, H. Elhouichet and A. Moadhen, "Yb^{3+} effect on the spectroscopic properties of Er-Yb codoped SnO_2 thin films", J. Luminen. **131**, 2630 (2011).
[18] H. Ahmad, K. Thambiratnam, M. C. Paul, A. Z. Zulkifli, Z. A. Ghani and S. W. Harun, "Fabrication and application of zirconia-erbium doped fibers", Opt. Mat. Express **2**, 1690 (2012).
[19] Y.-C. Huang, C.-N. Liu, Y.-S. Lin, J.-S. Wang, W.-L. Wang, F.-Y. Lo, T.-L. Chou, S.-L. Huang and W.-H. Cheng, "Fluorescence enhancement in broadband Cr-doped fibers fabricated by drawing tower", Opt. Express **21**, 4790 (2013).
[20] G. Brambilla, V. Pruneri and L. Reekie, "Photorefractive index gratings in SnO_2:SiO_2 Optical fibers", Appl. Phys. Lett. **76**, 807 (2000).
[21] L. Dong, J. L. Cruz, J. A. Tucknott, L. Reekie and D. N. Payne, "Strong photosensitive gratings in tin-doped phosphosilicate optical fibers", Opt. Lett. **20**, 1982 (1995).
[22] Z. C. Liu, H. R. Chen, W. M. Huang, J. L. Gu, W. B. Bu, Z. L . Hua and J. L. Shi, "Synthesis of a new SnO_2/mesoporous silica composite with room-temperature photoluminescence", Microporous and Mesoporous Mat. **89**, 270 (2006).
[23] Y. C. Wu, W. Hamd, E. Thune, A. Boulle, C. Rochas and R. Guinebretière, "Synthesis of tin oxide nanosized crystal embedded in silica matrix through sol-gel process using alkoxide precursors ", J. Non-Cryst. Solids **355**, 951 (2009).
[24] O. Masson, R. Guinebretière and A. Dauger, "Reflection asymmetric powder diffraction with flat-plate sample using a curved position-sensitive detector", J. Appl. Crystal. **29**, 540 (1996).
[25] T. Van Tran, S. Turell, M. Eddafi, B. Capoen, M. Bouazaoui, P. Roussel, S. Berneschi, G. Righini, M. Ferrari, S. N. B. Bhaktha, O. Cristini and C. Kinowski, "Investigations of the effects of the growth of SnO_2 nanoparticles on the strucural properties of glass-ceramic planar waveguides using Raman and FTIR spectroscopies", J. Mol. Struct. **976**, 314 (2010).
[26] C. D. S. Cunha, J. L. Ferrari, D. C. Oliveira, L. J. Q. Maia, A. S. L. Gomes, S. J. L. Ribeiro and R. R. Gonçalves, "NIR luminescent Er^{3+}/Yb^{3+} co-doped SiO_2-ZrO_2 nanostructured planar and channel waveguides: Optical and structural properties", Mat. Chem. Phys. **136**, 120 (2012).
[27] O. Humbach, H. Fabian, U. Grzesik, U. Haken and W. Heitmann, "Analysis of OH absorption bands in synthetic silica", J. Non-Cryst. Sol. **203**, 19 (1996).
[28] N. Chiodini, F. Morazzoni, A. Paleari, R. Scotti and G. Spinolo, "Sol-gel synthesis of monolithic tin-doped silica glass", J. Mater. Chem **9**, 499 (1999).
[29] V. G. Kravets, "Spectroellipsometric and photoluminescence studies of SnO_x structured doped with Sm ions", J. Allow. Comp. **509**, 8888 (2011).
[30] R. Lorenzi, A. Lauria, N. Mochenova, N. Chiodini and A. Paleari, "Study of the absorption edge of SnO_2 nanoparticles embedded in silica films", J. of Non-Cryst. Solids **357**, 1888 (2011).
[31] C. Xia, G. Zhou, Y. Han, X. Zhao and L. Hou, "Luminescence of Yb^{2+}, Yb^{3+} co-doped silica glass for white light source", Opt. Mater. **34**, 769 (2012).
[32] S. Rydberg and M. Engholm, "Experimental evidence for the formation of divalent ytterbium in the photodarkening process of Yb-doped fiber lasers", Opt. Express **21**, 6681 (2013).